Physica Scripta

INCLUSIVE PUBLISHING TRUSTED SCIENCE

PURPOSE-LED PUBLISHING™

PAPER • **OPEN ACCESS**

Thirring universe model

To cite this article: Nazmi Yılmaz *et al* 2024 *Phys. Scr.* **99** 105044

View the article online for updates and enhancements.

You may also like

- Mach, Thirring & Lense, Gödel–getting dizzy in space-time
Franz Embacher
- Lieb-Thirring integral inequalities and their applications to attractors of the Navier-Stokes equations
A A Il'in
- Lieb-Thirring inequalities on the torus
A. A. Ilyin and A. A. Laptev

This content was downloaded from IP address 88.255.99.31 on 14/03/2025 at 12:21

Physica Scripta

PAPER

Thirring universe model

Nazmi Yılmaz[1], Mahmut Akıllı[2] and K G Akdeniz[3]

[1] Koç University, College of Sciences, Department of Physics, Istanbul, Turkey
[2] Medical Imaging Techniques Program, Vocational School, Istanbul Arel University, Istanbul, Turkey
[3] Istanbul University, Istanbul, Turkey

E-mail: nayilmaz@ku.edu.tr

Keywords: thirring model, entropy, lyapunov exponents, chaos

OPEN ACCESS

RECEIVED
10 May 2024

ACCEPTED FOR PUBLICATION
11 September 2024

PUBLISHED
20 September 2024

Original content from this work may be used under the terms of the Creative Commons Attribution 4.0 licence.
Any further distribution of this work must maintain attribution to the author (s) and the title of the work, journal citation and DOI.

Abstract

In recent years, there has been a significant amount of research focused on Thirring instantons. This study aims to employ the Thirring quantum model as a theoretical Universe model to gain a more profound understanding of the beginning of the Universe. For this, we propose to analyze the entropy of the quantum states of zero energy Thirring instanton solutions and the transition to other quantum states. Our findings by also using Lyapunov exponents and the cyclic attractors as comparative nonlinear methods show that there is no entropy corresponding to instanton solutions with zero energy and that the sudden increase in entropy indicates the formation of the Universe. We evaluate the implications of this study in terms of the standard Universe model. Thus we anticipate that these results have the potential to contribute significantly to our understanding of the origin of the Universe and highlight the role of chaos and complexity in its evolution.

1. Introduction

As well known, the Thirring model stands as a quantum field theory construct that characterizes the correlation functions of $\bar{\psi}\psi$, a self-coupled Dirac field within a solitary spatial and temporal dimension. Its massless configuration marked by conformal symmetry, exhibits characteristics reminiscent of the quantized behaviour observed in relativistic quantum field theories [1–5]. Its instanton-type solutions, particularly its manifestation as a vacuum with zero energy $0|\bar{\psi}\psi|\ 0 \neq 0$, have undergone thorough examination [6, 7]. In a recent publication by two of the authors of this paper, Akıllı and Yılmaz, titled 'Entropy of the Quantum Fluctuations of Fermionic Instantons' (EQFFI) [8], the investigation explores the analysis of the emergence of fermions with the in the early stages of the Universe. Their study examines explicitly the entropy of quantum fluctuations within the massless Thirring model's instanton solutions [9–16], using the Boltzmann, Gibbs and Shannon (BGS) entropy of the quantized orbits. The results of EQFFI indicate that the initiation of the life of the Universe occurred in a low-entropy state, and the entropy of quantum fluctuations increased during the fermion creation.

In this paper, we seek to use the massless Thirring model as a theoretical basic Universe model to perform a detailed analysis of the change of entropy at the birth of the Universe, Thirring Universe. For this, we use calculations and comparisons involving scalogram entropy [17, 18], sample entropy [19], and Lyapunov exponents [20]. Additionally, we extract the phase orbits of Thirring instanton solutions.

We predict that the Thirring Universe model that we propose endeavours to offer a comprehensive insight into the entropy state at the inception of the Universe. We also anticipate that our study holds the potential to enhance our understanding of the Universe's origins and provides a fresh perspective on the conditions behind the creation of the first particles.

© 2024 The Author(s). Published by IOP Publishing Ltd.

1.1. The thirring model

Walter E. Thirring first described the Thirring model in 1958 using the Lagrangian density [21]

$$\mathscr{L} = \bar{\psi}(i\gamma^{\mu}\partial_{\mu})\psi - \frac{1}{2}(\bar{\psi}\gamma^{\mu}\psi)^2 \tag{1}$$

Where ψ is the Thirring spinor field, $\bar{\psi}$ is the Dirac adjoint of ψ, expressed as $\bar{\psi} = \psi^{\dagger}\gamma^0$ are Dirac gamma matrices. ∂_{μ} is the partial derivative with respect to the spacetime coordinate x^{μ}. g is the coupling constant which represents the strength of the interaction between fermions. It can have both positive and negative values.

Starting from the Lagrangian density $\mathcal{L} = 0$ in equation (1), let $X(s)$ and $\phi(s)$ be complex fields, where $X(s) = X_1(s) + iX_2(s)$ and $\varphi(s) = \varphi_1(s) + i\varphi_2(s)$ with, $X_1(s)$, $X_2(s)$, $\varphi_1(s)$ are $\varphi_2(s)$ being real fields. The resulting set of non-linear differential equation (2) [22] is derived using the complex form of the Euclidian configuration in the Heisenberg ansatz [23, 24];

$$2X(s) + 2s\frac{dX(s)}{ds} - \alpha[sX(s)^2 + \varphi(s)^2]\varphi(s) = 0 \tag{2a}$$

$$2\frac{d\varphi(s)}{ds} + \alpha[sX(s)^2 + \varphi(s)^2]X(s) = 0 \tag{2b}$$

Here $X(s)$ and $\varphi(s)$ are the wings of Heisenberg ansatz. The transformations below [24] are employed to deduce the dimensionless representation of the system [25]; $X(s) = As^{-\sigma}F(Z)$, $\varphi(s) = Bs^{-\tau}G(Z)$ and $Z = lns$, where $\sigma = \tau + \frac{1}{2}$, $\tau = \frac{1}{4}$ and $A^2 = B^2$.

$$2\frac{dF(Z)}{dZ} + \frac{1}{2}F(Z) - \alpha AB[F(Z)^2 + G(Z)^2]G(Z) = 0 \tag{3a}$$

$$2\frac{dG(Z)}{dZ} - \frac{1}{2}G(Z) + \alpha AB[F(Z)^2 + G(Z)^2]F(Z) = 0 \tag{3b}$$

Where A and B are constants and the functions $F(Z)$ and $G(Z)$ are dimensionless. For $\alpha AB = 1$, the equilibrium points of the non-linear differential equation (3) are calculated as $(-0.5,\ -0.5)$, $(0,\ 0)$ and $(+0.5,\ +0.5)$ [24]. These equilibrium points represent the stable fermionic instanton solutions by Akdeniz and Smailagiç [25, 26].

For adjusting the Thirring oscillator's frequency, we employed frequency transformation in equations (3a) and (3b).

Defining $Z = wz$, w is the angular frequency.

$$\frac{dF(wz)}{d(wz)} = \frac{1}{w}\frac{dF(wz)}{dz} = \frac{1}{w}\frac{dF_*(z)}{dz} \tag{4a}$$

$$\frac{dG(wz)}{d(wz)} = \frac{1}{w}\frac{dG(wz)}{dz} = \frac{1}{w}\frac{dG_*(z)}{dz} \tag{4b}$$

And,

$$\frac{2}{w}\frac{dF_*(z)}{dz} + \frac{1}{2}F_*(z) - \alpha AB[F_*(z)^2 + G_*(z)^2]G_*(z) = 0 \tag{5a}$$

$$\frac{2}{w}\frac{dG_*(z)}{dz} - \frac{1}{2}G_*(z) + \alpha AB[F_*(z)^2 + G_*(z)^2]F_*(z) = 0 \tag{5b}$$

Then;

$$\frac{dF(z)}{dz} = w\left(-\frac{1}{4}F(z) + \frac{\alpha AB}{2}[F(z)^2 + G(z)^2]G(z)\right) \tag{6a}$$

$$\frac{dG(z)}{dz} = w\left(\frac{1}{4}G(z) - \frac{\alpha AB}{2}[F(z)^2 + G(z)^2]F(z)\right) \tag{6b}$$

2. Methods

2.1. Boltzmann, gibbs and shannon entropy

The entropy in statistical thermodynamics, derived by Boltzmann and Gibbs, is closely linked to the microstates of a system [27, 28]. The introduction of statistical mechanics and information theory has further popularized the concept of entropy [29–32]. In information theory, Shannon introduced entropy, which is functionally equivalent to entropy concept in statistical thermodynamics. The Boltzmann, Gibbs and Shannon (BGS) entropy is written as:

$$S_{BGS} = -k\sum_{i=1}^{w} p_i ln p_i \tag{7}$$

Where k is a positive constant associated with entropy quantification. In the field of thermodynamics, k corresponds to the Boltzmann constant expressed as $k_B = 1.38\ 10^{-23}\frac{J}{K}$. In information theory, the constant k is equal to 1. p_i denotes the probability of the ith microstate in a system. W represents the total number of microstates in the system.

2.2. Quantum entropy

Johann von Neumann formulated quantum entropy in 1932 basing it on a density matrix ρ that characterises the probability aspect of a system in quantum mechanics. The entropy of a density matrix ρ is expressed through a formula akin to the Shannon entropy applied to a probability distribution [33–35]:

$$S(\rho) = -Tr(\rho \ln \rho) \tag{8}$$

Here, ρ represents the density matrix for a single particle after reduction and Tr is the trace of the matrix. Upon obtaining the spectral diagonalization of ρ,

$$\rho = \sum_i p_i |\psi^i\rangle \langle\psi^i| \tag{9}$$

ψ^i is orthonormal and $p_i > 0$. The equation (9) yields to the matrix below [6];

$$\rho \ln \rho = \begin{pmatrix} p_1 \ln p_1 & & & \\ & p_2 \ln p_2 & & \\ & & p_3 \ln p_3 & \\ & & & \ddots \end{pmatrix} \tag{10}$$

This matrix can also be expressed the same as the Shannon entropy corresponding to the probability distribution $\{p_i\}$, that satisfies $S(\rho) \geqslant 0$.

$$S(\rho) = -\sum_i p_i ln p_i \tag{11}$$

2.3. Scalogram entropy

The scalogram entropy [17, 18] is a method for calculating entropy based on wavelet scalograms. The wavelet scalogram, denoted as $S(s)$, represents the energy density distribution across different scales of a signal [36]. Considering a time series $f \in L^2\mathbb{R}$, over a finite time range, the inner scalogram is defined as follows;

$$S^{inner}(s) = Wf(u, s)_{J(s)} = \left(\int_{c(s)}^{d(s)} |Wf(u, s)|^2 du\right)^{1/2} \tag{12}$$

Here, $Wf(u, s)$ is the continuous wavelet transform of f at scale s and time u using a wavelet with compact support $\psi_{u,s}$ [36]. In quantitative analysis over a finite time interval I, wavelet function, $\psi_{u,s}$ is supported for all $u \in J(s)$, where the maximum subrange is $J(s) = [c(s), d(s)] \subseteq I$. The length of I should be chosen such that the function $J(s)$ is neither empty nor too small.

Comparison of different scales is facilitated by normalizing the inner scalogram [37];

$$\bar{S}^{inner}(s) = \frac{S^{inner}(s)}{(d(s) - c(s))^{\frac{1}{2}}} \tag{13}$$

The normalized inner scalogram gives the average of the energy density of the signal across all the scales without temporal information. The normalized inner scalogram yields a probability distribution p_s for a given time series f over scales from s_0 to s_1 can be given by [17, 18];

$$p_i = p_s = \frac{\bar{S}^{inner}(s)}{\sum_s \bar{S}^{inner}(s)} = (p_1, p_2, p_3, \ldots, p_s); \sum_s p_s = 1 \tag{14}$$

In this context, the distribution of probability is accomplished by partitioning the normalized inner scalogram at any given scale relative to the combined energy of the system. Thus, the resulting BGS entropy in equation (16) is defined as the scalogram entropy.

$$S'_{BGS} = -k\sum_s p_s \ln p_s \tag{15}$$

2.4. Sample entropy

Sample Entropy (SampEn) method [19] quantifies the disorder and complexity [38] within provided data [39–44]. It is the negative natural log of probability that two adjacent segments, each comprising m points, stay in proximity at the adjacent point, except the self-matching from the probability estimate. SampEn serves as a measure of self-similarity within a time series and remains unaffected by distortions stemming from self-matching. Notably, it demonstrates robustness across varying data lengths and proves useful in analyzing continuous time series. The expression for SampEn is as follows:

$$SampEn(m,\, r,\, N) = -ln\left(\frac{A}{B}\right) \tag{16}$$

where m is the data section length, N is the total length of the data and r represents the criterion for self-similarity. The terms A and B are defined below;

$$A = \left\{\frac{(N-m-1)(N-m)}{2}\right\}A^m(r),\; B = \left\{\frac{(N-m-1)(N-m)}{2}\right\}B^m(r) \tag{17}$$

Here $A^m(r)$ and $B^m(r)$ represent the probability of matching two segments for $m+1$ and m points respectively.

2.5. Lyapunov exponents

The Lyapunov exponent (LYP) serves as a metric to quantify the divergence of trajectories that were initially close to each other. With this information it helps determine how sensitive a system to its initial conditions and, consequently, the level of chaos within a system. In this study, the algorithm derived by Wolf *et al* [20] is employed for calculating Lyapunov exponent. The process begins by establishing a trajectory of reference, $\boldsymbol{X}(\boldsymbol{t}_0)$ and selecting its neighbouring trajectory, $\boldsymbol{Y}(\boldsymbol{t}_0)$ The distance between the two trajectories is denoted as $\boldsymbol{f}(\boldsymbol{t}_0) = \|\boldsymbol{X}(\boldsymbol{t}_0) - \boldsymbol{Y}(\boldsymbol{t}_0)\|$. Then the system is iterated multiple times, with the initial distance between the trajectory pair adjusted at each iteration. Subsequently, the degree of separation is calculated to determine the Lyapunov exponent.

$$\lambda = \frac{1}{t_N - t_0}\sum_{i=1}^{N}\log\frac{f(t_i)}{f(t_{i-1})} \tag{18}$$

Here λ represents the Lyapunov exponent and N is the iteration count applied to the system. The system is deemed chaotic when the Lyapunov exponent is a positive number [20, 45].

3. Results

We used fourth order Runge–Kutta algorithm to solve the dimensionless formulation of the massless Thirring model [46]. We obtained the fixed points corresponding to the instanton solutions [0.5, 0.5] and [−0.5, −0.5] for $\alpha AB = 1$ [21–26]. We then selected the fixed points as the initial conditions and determined $w = 100$ to obtain the numerical solutions of the equation (6) in the range of $1.001 \leqslant \alpha AB \leqslant 3$.

Figure 1(a) shows several cyclic attractors of the Thirring model in the range of $1.001 \leqslant \alpha AB \leqslant 1.100$ for the initial condition of [0.5, 0.5]. Figure 2(a) shows several cyclic attractors of the Thirring model in the range of $1 \leqslant \alpha AB \leqslant 3$ for the initial condition of [0.5, 0.5]. Figure 3(a) shows several cyclic attractors of the Thirring model in the range of $1 \leqslant \alpha AB \leqslant 3$ for the initial condition of [−0.5, −0.5].

Figure 1(b) indicates the largest Lyapunov exponent of the massless Thirring model calculated by increasing the αAB from 1.001 to 1.1 in steps of 0.001 for the initial condition of [0.5, 0.5] and $w = 100$. Figure 2(b) indicates the largest Lyapunov exponent of the massless Thirring model calculated by increasing the αAB from 1.1 to 3 in steps of 0.1 for the initial condition of [0.5, 0.5] and $w = 100$. Figure 3(b) indicates the largest Lyapunov exponent of the massless Thirring model calculated by increasing the αAB from 1.1 to 3 in steps of 0.1 for the initial condition of [−0.5, −0.5] and $w = 100$.

Figure 1(c) indicates the Sample entropy values of the massless Thirring model calculated by increasing the αAB from 1.001 to 1.1 in steps of 0.001 for the initial condition of [0.5, 0.5] and $w = 100$. Here, the tolerance r was selected as $r = 0.2_{*}std(data)$. Figure 2(c) indicates the Sample entropy values of the massless Thirring model calculated by increasing the αAB from 1.1 to 3 in steps of 0.1 for the initial condition of [0.5, 0.5] and $w = 100$. Figure 3(c) indicates the Sample entropy values of the massless Thirring model calculated by increasing the αAB from 1.1 to 3 in steps of 0.1 for the initial condition of [−0.5, −0.5] and $w = 100$.

Figure 1(d) indicates the Scalogram entropy values of the massless Thirring model calculated by increasing the αAB from 1.001 to 1.1 in steps of 0.001 for the initial condition of [0.5, 0.5] and $w = 100$. Here, the Haar–wavelet function with the integer scales in the range of $s_0 = 1$ and $s_1 = 256$ was used for scalogram entropy calculations. Figure 2(d) indicates the Scalogram entropy values of the massless Thirring model calculated by increasing the αAB from 1.1 to 3 in steps of 0.1 for the initial condition of [0.5, 0.5] and $w = 100$. Figure 3(d)

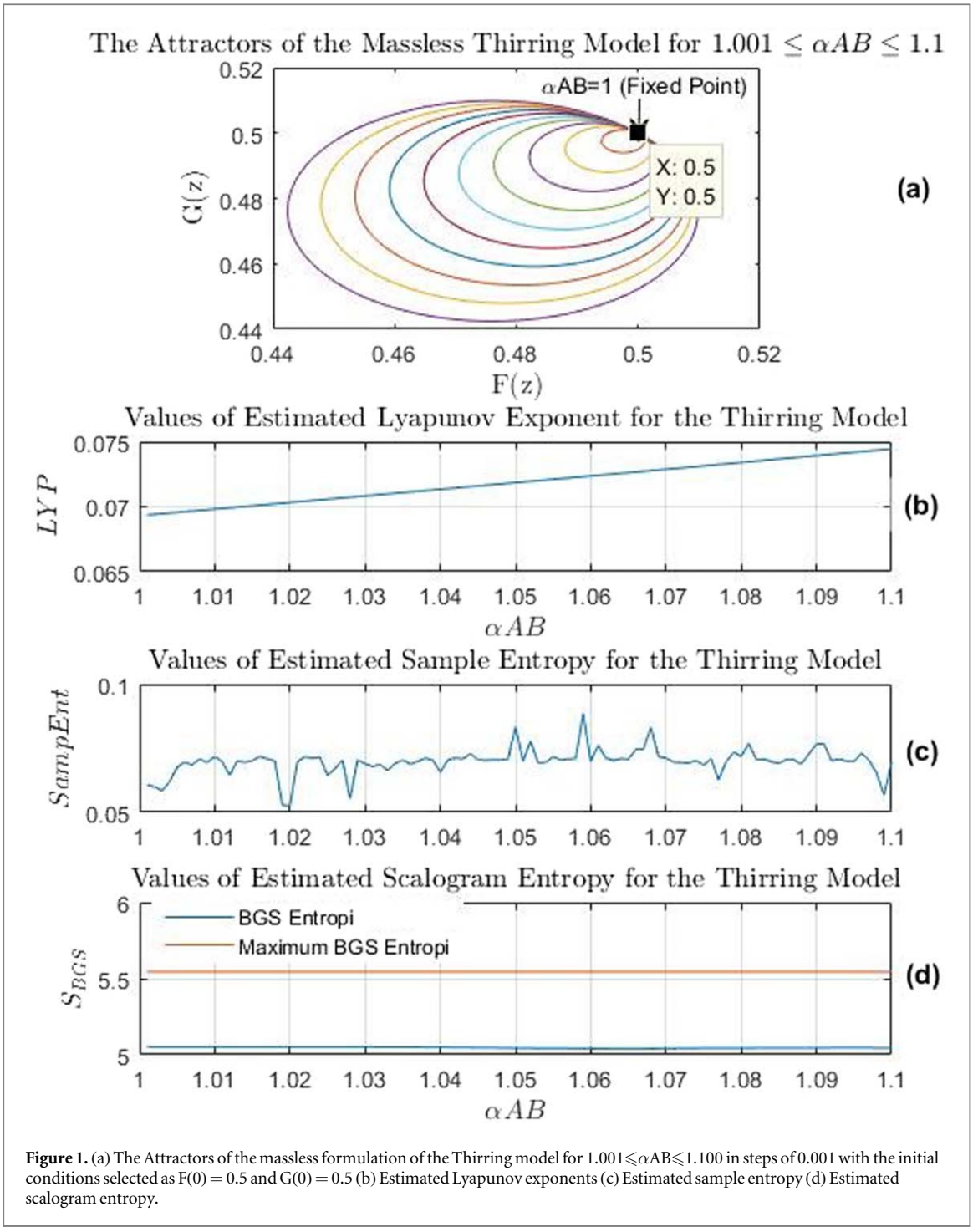


Figure 1. (a) The Attractors of the massless formulation of the Thirring model for 1.001⩽αAB⩽1.100 in steps of 0.001 with the initial conditions selected as F(0) = 0.5 and G(0) = 0.5 (b) Estimated Lyapunov exponents (c) Estimated sample entropy (d) Estimated scalogram entropy.

indicates the Scalogram entropy values of the massless Thirring model calculated by increasing the αAB from 1.1 to 3 in steps of 0.1 for the initial condition of $[-0.5, -0.5]$ and $w = 100$.

4. Discussion

The singularity at the beginning of the Universe and the initial stages of the Universe are marked by the creation of the first particles. Our study proposes that the initial particles formed by a sudden increase in entropy following a singular point with zero energy characterized by 'zuhur': unpredictable emergence [47]. This perspective offers a nuanced viewpoint, providing an alternative framework for exploring the beginning of the Universe.

We used the massless Thirring model as a theoretical Universe model to analyze the entropy at the birth of the Universe. Because, the Thirring model, being a construct of quantum field theory, particularly in its massless configuration, exhibits characteristics akin to the quantized behavior observed in relativistic quantum field

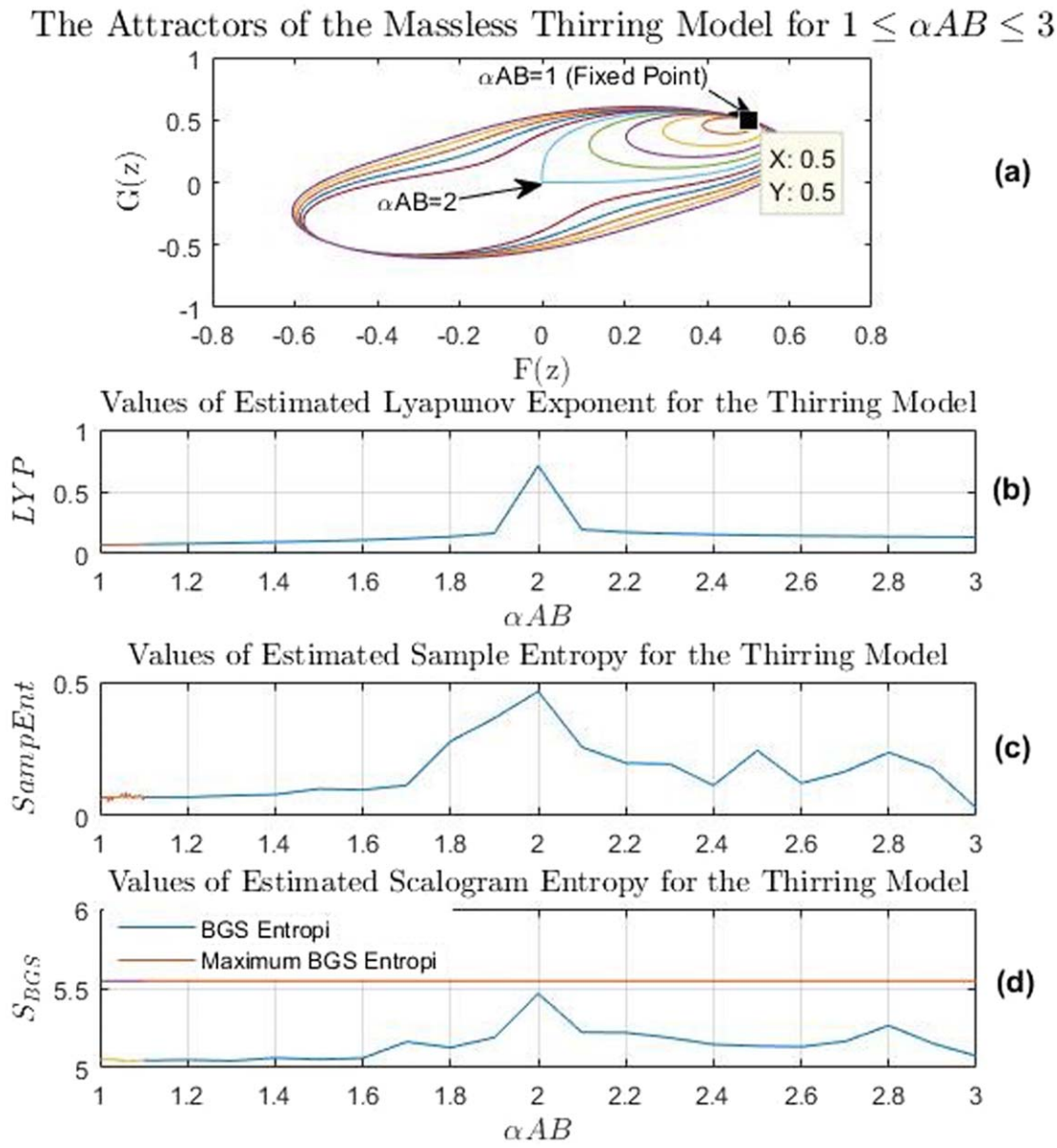


Figure 2. (a) The Attractors of the massless formulation of the Thirring model for $1 \leqslant \alpha AB \leqslant 3$ in steps of 0.1 with the initial conditions selected as $F(0) = 0.5$ and $G(0) = 0.5$. (b) Estimated Lyapunov exponents (c) Estimated sample entropy (d) Estimated scalogram entropy.

theories. Therefore, the creation of first particles can be analysed by the entropy of the massless Thirring model to simulate the early stages of the Universe.

Through examination of the entropy, Lyapunov exponents, and cyclic attractors of the massless formulation of the Thirring model, we propose the existence of a zero energy quantum state, referred to as 'zuhur,' behind the creation of fermions. Notably, the Thirring attractor demonstrates a fixed point solely in instanton solutions when $\alpha AB = 1$ as depicted in figure 1. At this fixed point, quantum fluctuations are absent, indicating that the frequency, hence the energy of this quantum state is zero, accompanied by the absence of entropy. Quantum fluctuations resume when the Thirring system undergoes slight change, approximately $\alpha AB \approx 1$, as illustrated in figure 1.

As shown in figures 2(a) and 3(a), The Thirring model exhibits periodic oscillations which have a monophasic waveform in the interval of $1 < \alpha AB \leqslant 2$. These periodic oscillations of the model slightly deteriorate for $\alpha AB = 2$. After this deterioration, the model transits from monophasic oscillations to biphasic oscillations. Their phase diagrams in the case of $\alpha AB > 2$ corresponds to the fermionic creation. Thus, the cyclic attractors in figures 2(a) and 3(a) indicate the fermion creation for $\alpha AB > 2$.

Considering energy-work conversion processes, which lead to an increase in entropy, we can interpret particle formation as a form of work, thus anticipating a subsequent rise in entropy. Figures 2(b)–(d) and 3(b)–(d) exhibit a sudden increase in entropy and Lyapunov exponent. In the phase where $1 < \alpha AB < 2$ and

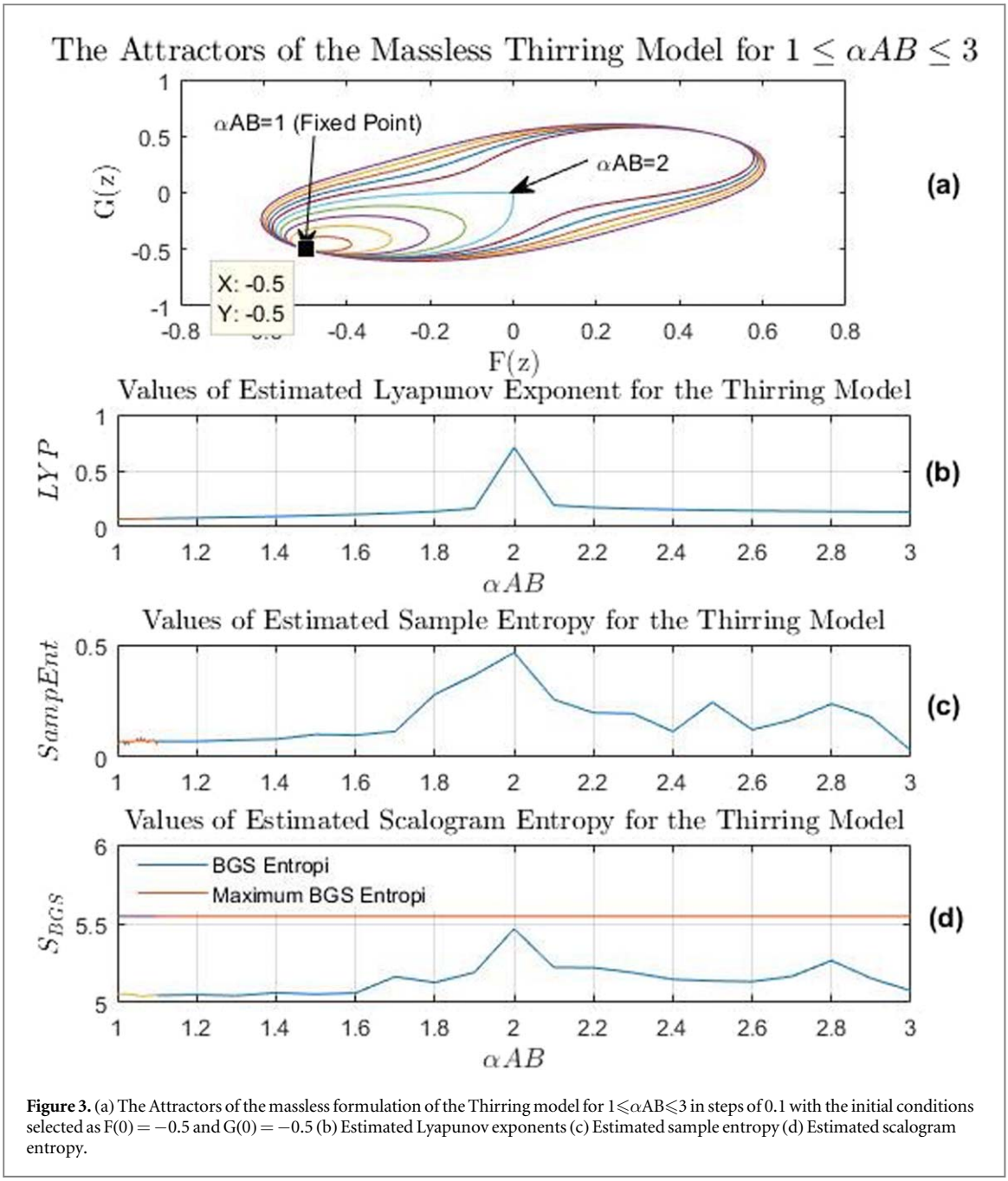


Figure 3. (a) The Attractors of the massless formulation of the Thirring model for $1 \leqslant \alpha AB \leqslant 3$ in steps of 0.1 with the initial conditions selected as $F(0) = -0.5$ and $G(0) = -0.5$ (b) Estimated Lyapunov exponents (c) Estimated sample entropy (d) Estimated scalogram entropy.

entropy remains stable, there is no discernible indication of particle creation, hence no evidence of Universe formation. However, at $\alpha AB = 2$, a sudden increase in entropy and Lyapunov exponents occurs, marking the initiation of the Universe. Consequently, we deduce that particles are generated following the zero energy state at $\alpha AB = 1$, thereby suggesting an inherent developmental dynamic of the Universe. This model works in harmony with the general assumption that the Universe begins in a state of low entropy.

To relate our findings to the works of Neil Turok, he modeled the emergence of an infinite open universe from a 'pea'-sized Hawking-Turok instanton. In his model, quantum fluctuations occur at this instanton of the metric tensor, with space-time inflation driven by quantum jumps uphill [48, 49]. Similarly, in our Thirring model, the state $\alpha AB > 2$, representing particle creation, corresponds to the quantum fluctuations of the Hawking-Turok instanton. We also believe our model, at the state $\alpha AB = 1$, reflects the pre-Hawking-Turok instanton of the Universe, providing a unique approach to exploring early universe dynamics.

Data availability statement

No new data were created or analysed in this study. The data that support the findings of this study are available upon reasonable request from the authors.

ORCID iDs

Nazmi Yılmaz https://orcid.org/0000-0002-0631-257X
Mahmut Akıllı https://orcid.org/0000-0002-8656-2594

References

[1] Coleman S R 1975 Quantum sine-gordon equation as the massive Thirring model *Rev.* D **11** 2088–97
[2] Birrell N D and Davies P C W 1978 Massless thirring model in curved space: thermal states and conformal anomaly *Phys. Rev.* D **18** 4408–21
[3] Carey A L, Ruijsenaars S N M and Wright J D 1985 Commun. the massless thirring model: positivity of klaiber's n-point functions *Math. Phys.* **99** 347–64
[4] Depireux D A, Gates S J and Park Q-H 1989 Lefton-righton formulation of massless thirring models *Phys. Lett.* B **224** 364–72
[5] Benfatto G, Falco P and Mastropietro V 2007 Commun. functional integral construction of the thirring model: axioms verification and massless limit *Math. Phys.* **273** 67
[6] Heisenberg W 1957 Z. naturforsch. quantum theory of fields and elementary particles *Rev. Mod. Phys.* **29** 269–78
[7] Yılmaz N, Canbaz B, Akıllı M and Onem C 2018 Study of the stability of the fermionic instanton solutions by the scale index method *Phys. Lett.* A **382** 2118
[8] Akıllı M and Yılmaz N 2022 Entropy of the quantum fluctuations of fermionic instantons in the universe *Modern Physics Letters* A **37** 2250101
[9] Volovik G E 1997 Fermionic entropy of the vortex state in d-wave superconductors *JETP Lett.* **65** 491
[10] Wolf M M 2006 Violation of the Entropic Area Law for Fermions *Phys. Rev. Lett.* **96** 010404
[11] Gioev D and Klich I 2006 Entanglement entropy of fermions in any dimension and the widom conjecture *Phys. Rev. Lett.* **96** 100503
[12] Stafford C A and Shastry A 2017 Local entropy of a nonequilibrium fermion system *J. Chem. Phys.* **146** 092324
[13] Sun Y and Sun J-R 2019 Note on the rényi entropy of 2D perturbed fermions *Phys. Rev.* D **99** 106008
[14] Mamaev M, Kimchi I, Perlin M A, Nandkishore R M and Rey A M 2019 *Phys. Rev. Lett.* **123** 130402
[15] Bueno P and Casini H 2020 Reflected entropy, symmetries and free fermions *J. High Energy Phys.* **2020** 103
[16] Plastino A and Rocca M C 2020 Quantization of Newton's gravity *Ann. Phys.* **412** 168013
[17] Akıllı M, Yılmaz N and Akdeniz K G 2019 Study of the q-Gaussian distribution with the scale index and calculating entropy by normalized inner scalogram *Phys. Lett.* A **383** 1099–104
[18] Akıllı M, Yılmaz N and Akdeniz K G 2021 The 'wavelet'entropic index q of nonextensive statistical mechanics and superstatistics *Chaos, Solitons Fractals* **150** 111094
[19] Richman J S and Moorman J R 2000 Physiological time-series analysis using approximate entropy and sample entropy *Am. J. Physiol. Heart Circ. Physiol.* **278** H2039–49
[20] Wolf A *et al* 1985 Determining lyapunov exponents from a time series *Physica* D **16** 285–317
[21] Thirring W E 1958 A soluble relativistic field theory *Ann. Phys.* **3** 91
[22] Canbaz B, Onem C, Aydogmus F and Akdeniz K G 2012 From heisenberg ansatz to attractor of thirring instanton *Chaos Solitons Fractals* **45** 188
[23] Heisenberg W 1954 Z. naturforsch. zur quantentheorie nichtrenormierbarer wellengleichungen *Z. Naturforsch.* A **9** 292
[24] Kortel F 1956 On some solutions of gursey's conformal-invariant spinor wave equation *II Nuovo Cimento* **4** 210–5
[25] Akdeniz K G and Hortacsu M 1980 Functional determinant for the thirring model with instanton *II Nuova Cimento* A **59** 181
[26] Akdeniz K G and Smailagic A 1979 Classical solitons for fermionic models *Nuovo Cimento* A **51** 345–57
[27] Gibbs J W 1902 *Elementary Principles in Statistical Mechanics* (C. Scribner's Sons)
[28] Shannon C E 1948 A mathematical theory of communication *Bell Syst Tech J;* **27** 379–423
[29] Jaynes E T 1957 Information theory and statistical mechanics *Phys. Rev.* **620** 106
[30] Penrose O 1970 *Foundations of Statistical Mechanics: A Deductive Treatment* (Pergamon)
[31] Beck C and Cohen E G D 2003 Superstatistics *Condensed Matters* **322** 0205097
[32] Gray R M 2009 *Entropy and Information Theory* (Springer)
[33] von Neumann J 2013 *Mathematische Grundlagen Der Quantenmechanik* Vol. 38 (Springer)
[34] Nikouravan B 2019 Int. J. fundam. von neumann entropy by logarithmic method *Phys. Sci.* **9** 55
[35] Witten E 2020 A mini-introduction to information theory *Riv. del Nuovo Cimento* **43** 187
[36] Mallat S 1999 *A Wavelet Tour of Signal Processing* (Elsevier)
[37] Benitez R, Bolos V J and Ramirez M E 2010 A wavelet based tool for studying non-periodicity *Comput. Math. Appl.* **60** 634–41
[38] Yılmaz N, Akıllı M and Akdeniz K G 2020 A new method in the analysis of chaotic systems: scale index *Springer Proceedings in Complexity* (Springer) 21–6
[39] Acharya U R, Molinari F, Sree S V, Chattopadhyay S, Ng K-H and Suri J S 2012 Automated diagnosis of epileptic EEG using entropies *Biomed. Signal Process. Control* **7** 401–8
[40] Yentes J M, Hunt N, Schmid K K, Kaipust J P, Mcgrath D and Stergiou N 2013 The appropriate use of approximate entropy and sample entropy with short data sets *Ann. Biomed. Eng.* **41** 349–65
[41] Delgado-Bonal A and Marshak A 2019 Approximate entropy and sample entropy: a comprehensive tutorial *Entropy* **21** 541
[42] Jia Y and Gu H 2019 Identifying nonlinear dynamics of brain functional networks of patients with schizophrenia by sample entropy *Nonlinear Dyn.* **96** 2327–40
[43] Marques J A L, Cortez P C, Madeiro J P V, de Albuquerque V H C, Fong S J and Schlindwein F S 2020 Nonlinear characterization and complexity analysis of cardiotocographic examinations using entropy measures *J. Supercomput.* **76** 1305–20
[44] Wang F, Zhao W and Jiang S 2020 Detecting asynchrony of two series using multiscale cross-trend sample entropy *Nonlinear Dyn.* **99** 1451–65
[45] Strogatz S G 1994 *Nonlinear Dynamics and Chaos: with Applications to Physics, Biology, Chemistry and Engineering* (Addison-Wesley)
[46] Griffiths D F and Higham D J 2010 *Numerical Methods for Ordinary Differential Equations* (Springer)
[47] Akdeniz K G 2010 Disorder in complex human system *Proceedings of the Conference in Honour of Murray Gell-Mann's 80th Birthday Quantum Mechanics, Elementary Particles, Quantum Cosmology and Complexity* ed H Fritzsch and K K Phua (World Scientific Publishing) 630–7
[48] Turok N and Hawking S W 1998 Open inflation, the four form and the cosmological constant *Phys. Lett.* B **432** 271–8
[49] Turok N 2001 Inflation and the beginning of the universe *Ann. N.Y. Acad. Sci.* **950** 83–96